X-ray Structure of the Carboplatin-Loaded Apo-Ferritin Nanocage

DOI:
10.1021/acsmedchemlett.7b00025

Document Version
Accepted author manuscript

X-ray Structure of the Carboplatin-loaded Apo-Ferritin nanocage

Nicola Pontillo,[a] Giarita Ferraro,[a] John R. Helliwell,[b] Angela Amoresano,[a] and Antonello Merlino[a,c*]

[a]Department of Chemical Sciences, University of Naples Federico II, Complesso Universitario di Monte Sant'Angelo, Via Cintia, I-80126, Napoli, Italy. Tel: +39081674276; Fax: +39081674090; E-mail: antonello.merlino@unina.it

[b]School of Chemistry, Faculty of Engineering and Physical Sciences, University of Manchester, Brunswick Street, Manchester M13 9PL, England

[c]CNR Institute of Biostructures and Bioimages, Via Mezzocannone 16, I-80126, Napoli, Italy

KEYWORDS: Pt-based drugs, carboplatin, ferritin, encapsulated drugs

ABSTRACT: The second-generation Pt anticancer agent carboplatin (CBDCA) was encapsulated within apo horse spleen ferritin (AFt) nanocage and the X-ray structure of the drug-loaded protein was refined at 1.49 Å resolution. Two Pt binding sites, different from the one observed in the cisplatin-encapsulated AFt, were identified in Ft subunits by inspection of anomalous electron density maps at two wavelengths and difference Fourier electron density maps, which provide the necessary sensitivity to discriminate between Pt from CBDCA and Cd ions that are present in the crystallization conditions. Pt centres coordinate to the NE2 atom of His49 and to the NE2 atom of His132, both on the inner surface of the Ft nanocage.

Platinum-based drugs cisplatin (CDDP), carboplatin (CBDCA) and oxaliplatin were approved for medical treatment of cancer by the FDA and are in widespread use [1-11]. Although some of the main side effects of CDDP for cancer patients were alleviated using the second-generation Pt-based drugs CBDCA and oxaliplatin, the clinical use of these important anticancer agents is still greatly hampered by high systemic toxicity and by common Pt compound resistance processes[9-11]. Improving the delivery of these drugs is therefore very important for their biomedical application. In the last few years considerable efforts were put into the development of Pt-based drug vectors (e.g. liposomes, copolymers, dendrimers, inorganic and organic macrocycles and nanoparticles) that could reduce these toxicity and resistance problems[12-14]. The most desirable vectorial systems for these purposes are obviously biocompatible materials, like protein-based nanoparticles[15-17].

Among the systems used to enhance the delivery of Pt-based drugs, the case of the iron-storage protein ferritin (Ft) is very interesting and obviously appropriate[18-22]. Mammalian Fts are heterogeneous: they consist of two subunits, called heavy (H) and light (L) protein chains due to their different molecular weights (~21 and ~19 kDa, respectively), as well as of different primary amino acid sequence and also function[23]. In vertebrates, Ft is assembled from 24 chains into a spherical cage (~8 and 12 nm of inner and outer diameter, respectively). Each protein subunit folds as a four-helix bundle. The 24 four helix bundle subunits form an octahedral structure 'nanocage' with 432 point group symmetry [24-26]. This Ft nanocage can incorporate up to 4500 atoms of Fe [24-26].

Human Ft is very promising as a Pt-based drug loading and releasing system since it is non-immunogenic and biocompatible[27], it is highly stable and soluble in the bloodstream, it can be internalized via Ft-binding receptors (like transferrin receptor 1, which specifically recognizes H-chains, or Scara5 that binds L-chains[28]), which are over-expressed in a variety of malignant cells[28-31], and it has a long circulation half-life[32]. It was demonstrated that Ft binds at the gastric cancer cell (GCC) membrane surface, thus it is likely that Ft could efficiently enter cells[20-22,31]. Iron oxide rich ferritin nanoparticles have been used to target and visualize tumour tissues without the use of additional contrast agents.[33] Furthermore, it is possible to manipulate the Ft surface genetically or chemically so that it can efficiently and selectively recognize tumour cells through interactions with overexpressed integrin $\alpha v\beta 3$[34].

Fts from various sources were previously exploited to encapsulate doxorubicin[35] ,CDDP, CBDCA, oxaliplatin, and other metal-based drugs[36-40].

Up to 55 molecules of CDDP and up to 120 molecules of CBDCA can be entrapped in each Ft nanocage[36-39]. Cytotoxicity of the encapsulated drug-AFt adducts was evaluated on different tumor cell lines[36-39].

We recently reported the high resolution X-ray structure of CDDP-encapsulated apo (AFt) horse spleen ferritin (L-chain)[40]. Our data demonstrated that CDDP is trapped within the cage close to the ND1 atom of His132 and that the outer surface of AFt is unaltered upon CDDP encapsulation[40], thus suggesting that the drug-loaded protein remains highly biocompatible and able to transport the drug to malignant cells.

The structure of CBDCA-encapsulated AFt is unknown and the reason for the different amount of Pt complex encapsulated in AFt remains to be determined.

Here, we report the determination of the X-ray crystal structure of CBDCA-encapsulated AFt at 1.49 Å resolution using the European Synchrotron Radiation Facility (ESRF, Grenoble, France).

Encapsulation of Pt inside the Ft cage was obtained by first disassembling the cage into subunits at pH=13 and then reconstituting it at neutral pH, as was done to encapsulate CDDP in AFt[40]. The encapsulation was performed using the same batch of protein that was used to prepare CDDP-encapsulated AFt[40]. Specifically, a protein sample of concentration 20 mg x mL^{-1} was first dissociated at pH 13 in the presence of CBDCA (thus the Ft subunit to metal drug ratio used is in the range 1:30 to 1:280) and then reassembled at neutral pH.

The CBDCA incorporation was confirmed by inductively coupled plasma mass spectrometry (ICP-MS) studies. These mass data indicate that the amount of Pt encapsulated in AFt depends on the preparation and on the protein to metal molar ratio that are used to obtain the adduct. Starting from a protein subunit to metal molar ratio of 1:30, a range from 25 to 82 atoms of Pt can be encapsulated within the cage. Starting from a protein subunit to metal ratio of 1:280, we were able to incorporate up to 144 Pt atoms within the cage (6 Pt atoms per Ft subunit). This value is higher than that found in the literature, where a CBDCA fragment/Ft cage molar ratio between 17 and 120 was observed[36,39]. The protein to metal ratio value that we have observed is significantly higher than those that were found for CDDP (Pt/Ft cage ratio between 11.2 and 55)[36,39, 40].

As observed for CDDP-encapsulated AFt[40], CBDCA-encapsulated AFt does not contain Fe.

The Ft conformation in the CBDCA-encapsulated AFt was evaluated by comparing its far-UV circular dichroism spectrum with that of the native protein used as control[40] (Figure S1). Spectra show very similar curves, confirming that the encapsulation of the drug does not affect the secondary structure of the protein.

Crystals of CBDCA-encapsulated AFt were grown using a sample of the adduct, characterized as detailed above by the presence of up to 144 atoms of Pt within the protein cavity (i.e. 6 Pt for Ft subunits). Crystals are isomorphous to those obtained for CDDP-encapsulated AFt (PDB code 5ERJ) and for the native protein used as control (PDB code 5ERK). X-ray diffraction data were first collected at 1.96 Å resolution at the CNR Institute of Biostructures and Bioimages in Napoli, Italy, using a CuKα radiation and then recollected at higher resolution (1.49 Å) at ESRF synchrotron using a 0.9677 Å wavelength (Table S1). The structure of CBDCA-encapsulated AFt (Figure 1A) was solved by the difference Fourier method using the coordinates of the native Ft (control) crystallized under the same experimental conditions and determined at 2.00 Å resolution in our laboratory, as starting model (PDB code 5ERK)[40]. The best structure of CBDCA-encapsulated AFt (Figure 1A), solved at 1.49 Å resolution, includes 1782 non-H atoms, 4 Pt atoms in two different binding sites, 11 Cd^{2+} ions, a sulphate ion, four Cl^- and refines to an R-factor of 0.158 (R-free=0.181) (see SI for further details).

As expected, superimposition of the structure of CBDCA-encapsulated AFt to that of native Ft used as starting model results in nearly identical protein structures with a root mean square deviation (rmsd) of 0.40 Å for alpha carbon atoms. A detailed comparison with the structure of CDDP-encaspulasted AFt is reported in S.I. In CBDCA-encapsulated AFt each protein subunit adopts a four-helix bundle constituted by helices A, B, C and D and an additional short helix (helix E) at the C-terminus. As usual 24 monomers assemble in an octahedral structure (432 point group symmetry) that form the hollow cage (Figure 1B).

To discriminate between Pt and Cd ions from crystallization conditions, anomalous electron density maps calculated at each of the two different X-ray wavelengths were compared. By comparison between CuKα (1.5418Å) and the wavelength used at ESRF (0.9677Å), the Cd and the Pt f'' signals change in opposite ways providing an exquisite sensitivity to discriminate between these two chemical elements. In particular, if one considers the f'' values of these two atoms at these two wavelengths it is possible to note that the Pt signal increases from about 7 electrons to 9 electrons and the Cd signal drops from 4.7 electrons to 2 electrons going from CuKα to 0.9677 Å X-ray wavelength. Thus, the direct comparison of each of the anomalous difference Fourier electron density map peaks at the two wavelengths elegantly reveals which peaks should be attributed to Pt and which ones to Cd. The comparison between the anomalous peak signals of Cd and Pt atoms are reported in Table 1, together with the assignments made and the comparison with the interpretation of the same peaks in the control study. Interestingly, these data show the presence of two Pt binding sites: one is close to the NE2 atom of His49, which adopts two distinct conformations in both the structures of CBDCA-encapsulated AFt and in the control (Figure 2C-D and in Figure S2). The second is close to the NE2 atom of His132 (Figure 2E-F and in Figure S2). The ND1 atom of His132 was previously identified as a Pt binding site in the structure of CDDP-encapsulated AFt[40]. As observed when CDDP reacts with AFt, the Pt binding sites are partially occupied (0.3) and are located in the inner surface of the cage[40]. Although there is residual electron density close to the Pt centres, it is not sufficiently clear to make an assignment and thus the Pt ligands remain elusive. The inability to observe the Pt ligand of carboplatin upon interaction with proteins seems a general feature, since it has been a challenge reported by Tanley et al 2014 in their extensive survey of crystallisation conditions of lysozyme-carboplatin adducts[41,42] and by Messori et al. in 2015 in the X-ray structure of the adduct formed in

the reaction between carboplatin and bovine pancreatic ribonuclease (RNase A)[43]. Close to one of the two His49 conformers, a Pt atom interacts also with the side chain of Glu45 (Figure 2C). Interestingly, the electron density close to the His132 side chain and close to the other conformation of the His49 side chain is reminiscent of that observed in the X-ray structure of the adduct formed in the reaction between hen egg white lysozyme and CBDCA[41,42]. It is also interesting to note that CBDCA binding to His side chains has already been observed in the crystal structure of the adduct that the drug forms with RNase A[43]. His side chains have been also found frequently in the adduct that cisplatin and other Pt-based drugs form with proteins[44-48].

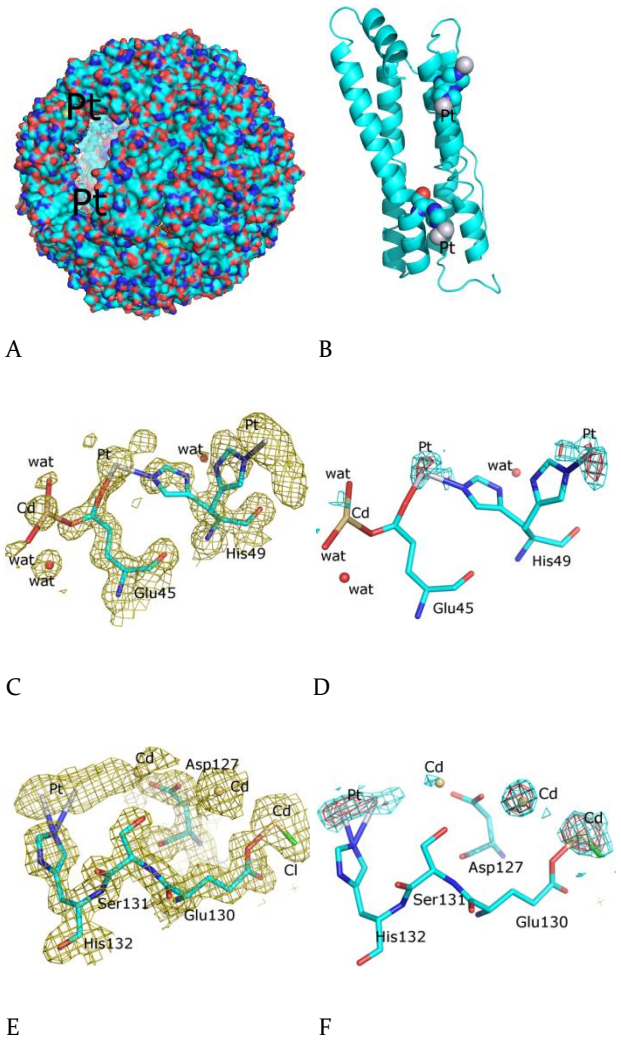

Figure 1. Overall structure of CBDCA-encapsulated AFt (panel A) and of a single CBDCA-encapsulated AFt subunit (panel B). In panel A, one Ft monomer was omitted, to allow the visualization of the Pt binding sites that are located in the inner surface of the cage. The Pt atoms are depicted as grey spheres. Stick model schematic representations of the Pt binding sites in the CBDCA-encapsulated AFt are reported in panels C-E. In these panels, 2Fo-Fc electron density maps of the adduct are contoured at 1.0 rms and reported in an olive colour. In panels D and F, the anomalous difference electron density map measured at the X-ray wavelength of 0.9677 Å and contoured at 2.0 and 3.0 σ, in cyan and red colours, respectively, is displayed.

Although Ft is believed to be a very good delivery system for antitumor metallodrugs[27-32], structural features of drug-loaded Ft systems were rarely investigated. Here, carboplatin was encapsulated within the ferritin nanocage and the structure of the adduct was characterized by X-ray crystallography. As observed for CDDP[40], the binding does not perturb the overall Ft structure and the charge of the protein surface and thus should not alter its biological action, an important feature as we have stressed in our introduction.

TABLE 1. Comparison of anomalous peak intensity in the structures of CBDCA-encapsulated AFt**.**

	CBDCA-encapsulated AFt		Assignment in CBDCA-encapsulated AFt
Source	ESRF λ=0.9677 Å	CuKα λ=1.5418 Å	
Resolution	1.50 Å	1.96 Å	
PDB code	5MIJ	5MIK	5MIJ
Atom in 5ERK	e/Å^3	e/Å^3	
CD 1. Close to Glu11	0.05	0.22	Cd^{2+}
CD 2. Close to Glu53/Glu56	0.12	0.22	Cd^{2+}
CD 3. Close to Glu60	0.20	0.25	Cd^{2+}
CD 4. At the binary axis. Close to Asp80	0.80	1.08	Cd^{2+}
CD 5. Close to Glu88	0.08	0.12	Cd^{2+}
CD 7. Close to His132	0.17	< 0.04	Pt^{2+} (PT 2)
CD 8. At the ternary axis. Close to Glu130	0.29	0.39	Cd^{2+}
CD 9. Close to His114	0.05/0.05	0.08/0.09	Cd^{2+}
CD 11. Close to Cys48	0.04	0.16	Cd^{2+}
CD 12. Close to Glu45	< 0.04	0.12	Cd^{2+}
CD 19. Not observed in the control. Close to Glu45	0.08	0.13	Cd^{2+}
CD 20 Not observed in the control. Close to Asp127	0.16	0.35	Cd^{2+}
Pt close to His49	0.17/0.17	< 0.04/0.13	Pt^{2+} (PT 1)

The platinum compound binding sites are located on the inner surface, close to the side chains of His132 and His49, which are residues that are also involved in the recognition of other metals, like Cd^{2+}. The apparent inconsistency between the amount of Pt determined by ICP-MS and the Pt binding sites derived by X-ray diffraction study can be easily explained considering that a large amount of carboplatin could be inside the cage, not coordinated to the protein, but just trapped in the bulk. The binding sites of CBDCA are different when compared to that observed for

CDDP. The existence of different binding sites for the two compounds supports the previous hypothesis that Pt ligands are responsible for the driving and identification of protein binding sites[46-47]. These results also indicate that it is in principle possible to obtain a mixed Pt-based drug encapsulated AFt, i.e. a protein cage with both CDDP and CBDCA bound in the core of the protein, as done for the bis-adduct formed in the competitive reaction between cisplatin and oxaliplatin with hen egg white lysozyme, where the two Pt-based drugs are concomitantly bound to the protein[48].

ASSOCIATED CONTENT

Supporting Information

Methods. Sample preparation and preliminary characterization. Crystallization, X-ray diffraction data collections, structure solution and refinement. Discrimination between Cd^{2+} and Pt^{2+}. Comparison with CDDP-encapsulated AFt. This material is available free of charge via the Internet at http://pubs.acs.org.

AUTHOR INFORMATION

Corresponding Author

*Antonello Merlino, Department of Chemical Sciences, University of Naples Federico II, via cintia, I-80126, Napoli, Italy. Phone: +39081674276, Fax:+39081674090, E-mail: antonello.merlino@unina.it

ORCID

Antonello Merlino: 0000-0002-1045-7720

Author Contributions

The manuscript was written through contributions of all authors.

Notes

The authors declare no competing financial interest.

ACKNOWLEDGMENT

We thank G. Sorrentino and M. Amendola for technical assistance during X-ray diffraction data collection at the IBB, Naples, Italy, M. Caterino for his help at ESRF and F. Pane for her help with ICP-MS.

ABBREVIATIONS

AFT, apoFerritin; CBDCA, carboplatin; CDDP, cisplatin; Ft, ferritin, ICP-MS, inductively coupled plasma mass spectrometry; RNase A, bovine pancreatic ribonuclease

REFERENCES

(1) Wang, D.; Lippard, S. J. Cellular processing of platinum anticancer drugs. *Nat. Rev. Drug Discov.* **2005**, *4*, 307-320.

(2) Kelland, L. The resurgence of platinum-based cancer chemotherapy. *Nat. Rev. Cancer* **2007**, *7*, 573-584.

(3) Sanderson, B.J.S.; Ferguson, L.R.; Denny, W.A. Mutagenic and carcinogenic properties of platinum-based anticancer drugs. *Mutat. Res-Fundam. Mol. Mech. Mut*. **1996**, 355, 59–70.

(4) Todd, R.C.; Lippard, S.J. Inhibition of transcription by platinum antitumor compounds. *Metallomics*. **2009**, *1*, 280-291.

(5) Raymond, E.; Faivre, S.; Chaney, S.; Woynarowski, J.; Cvitkovic, E. Cellular and molecular pharmacology of oxaliplatin. *Mol. Cancer Ther.* **2002**, *1*, 227–235.

(6) Green, M.H. *J.* Is cisplatin a human carcinogen? *Nat. Cancer Inst.* **1992**, *84*, 306–312.

(7) Zhai, X.; Beckmann, H.; Jantzen, H.M.; Essigmann, J. M. Cisplatin-DNA adducts inhibit ribosomal RNA synthesis by hijacking the transcription factor human upstream binding factor. *Biochemistry* **1998**, *37*, 16307–16315.

(8) Siddik, Z. H. Cisplatin: mode of cytotoxic action and molecular basis of resistance. *Oncogene* **2003**, *22*, 7265–7279.

(9) Go, R. S.; Adje, A.A. Review of the comparative pharmacology and clinical activity of cisplatin and carboplatin. *J. Clin. Oncol.* **1999**, *17*, 409-422.

(10) Holzer, A. K.; Manorek, G. H.; Howell, S. B. Contribution of the major copper influx transporter CTR1 to the cellular accumulation of cisplatin, carboplatin, and oxaliplatin. *Molec. Pharmacol.* **2006**, *70*, 1390–1394.

(11) Harrap, K. R. Preclinical studies identifying carboplatin as a viable cisplatin alternative. *Cancer Treat. Rev.* **1985**, *12*, 21–33.

(12) Rice, J. R.; Gerberich, J. L.; Nowotnik, D. P.; Howell, S. B. Preclinical efficacy and pharmacokinetics of AP5346, a novel diaminocyclohexane-platinum tumor-targeting drug delivery system. *Clin. Cancer Res.* **2006**, *12*, 2248-2254.

(13) White, S. C.; Lorigan, P.; Margison, G. P.; Margison, J. M.; Martin, F.; Thatcher, N.; Anderson, H.; Ranson, M. Phase II study of SPI-77 (sterically stabilised liposomal cisplatin) in advanced non-small-cell lung cancer. *Br. J. Cancer* **2006**, *95*, 822-828.

(14) Parker, J. P.; Ude, Z.; Marmion, C. J. Exploiting developments in nanotechnology for the preferential delivery of platinum-based anti-cancer agents to tumours: targeting some of the hallmarks of cancer. *Metallomics*, **2016**, *8*, 43-60.

(15) Zhen, Z.; Tang, W.; Zhang, W.; Xie, J. Folic acid conjugated ferritins as photosensitizer carriers for photodynamic therapy. *Nanoscale* **2015**, *7*, 10330-10333.

(16) Zhen, Z.; Tang, W.; Guo, C.; Chen, H.; Lin, X.; Liu, G.; Fei, B.; Chen, X.; Xu, B.; Xie, J. Ferritin nanocages to encapsulate and deliver photosensitizers for efficient photodynamic therapy against cancer. *ACS Nano* **2013**, *7*, 6988–6996.

(17) Maham, A.; Tang, Z.; Wu, H.; Wang, J.; Lin, Y. Protein-based nanomedicine platforms for drug delivery. *Small* **2009**, 5, 1706-1721.

(18) Zhen, Z.; Tang, W.; Todd, T.; Xie, J. Ferritins as nanoplatforms for imaging and drug delivery. *Expert Opin. Drug Deliv.* **2014**, *11*, 1913-1922.

(19) Heger, Z.; Skalickova, S.; Zitka, O.; Adam, V.; Kizek, R. Apoferritin applications in nanomedicine. *Nanomedicine* **2014**, *9*, 2233-2245.

(20) Uchida, M.; Flenniken, M.L.; Allen, M.; D. Willits, A.; Crowley, B. E.; Brumfield, S.; Willis, A. F.; Jackiw, L.; Jutila, M.; Young, M. J.; Douglas, T. Targeting of cancer cells with ferrimagnetic ferritin cage nanoparticles. *J. Am. Chem. Soc.* **2006**, *128*, 16626-16633.

(21) Yan, F.; Zhang, Y.; Yuan, H. K.; Gregas, M. K.; Vo-Dihn, T. Apoferritin protein cages: a novel drug nanocarrier for photodynamic therapy. *Chem. Comm*. **2008**, *38*, 4579-4581.

(22) Truffi, M.; Fiandra, L.; Sorrentino, L.; Monieri, M.; F. Corsi, S. Mazzucchelli. Ferritin nanocages: A biological platform for drug delivery, imaging and theranostics in cancer. *Pharmacol. Res.* **2016**, *107*, 57-65.

(23) Stefanini, S.; Chiancone, E.; Arosio, P.; Finazzi-Agro, A.; Antonini, E. Structural heterogeneity and subunit composition of horse ferritins. *Biochemistry* **1982**, *21*, 2293-2299.

(24) A.K. Powell, in: A. Sigel, H. Sigel (Eds.), Metal Ions in Biological Systems, vol. 35, Marcel Dekker, New York, 1998, pp. 515–561, and references therein.

(25) Andrews, S. C.; Arosio, P.; Bottke, W.; Briat, J. F.; von Darl, M.; Harrison, P. M.; Laulhere, J. P.; Levi, S.; Lobreaux, S.; Yewdall,

S. J. Structure, function, and evolution of ferritins. *J. Inorg. Biochem.* **1992**, *47*, 161–174.

(26) Zhang, Y.; Orner. B. P. Self-assembly in the ferritin nanocage protein superfamily. *Int. J. Mol. Sci.* **2011**, *12*, 5406-5421.

(27) Yang, Z.; Wang, X.; Diao, H.; Zhang, J.; Li, H.; Sunc, H.; Guo, Z. Encapsulation of platinum anticancer drugs by apoferritin. *Chem.Commun*. (Camb) **2007**, 3453-3455.

(28) Högemann-Savellano, D.; Bos, E.; Blondet, C.; Sato, F.; Abe, T.; Josephson, L.; Weissleder, R.; Gaudet, J.; Sgroi, D.; Peters, P. J.; Basilion, J. P. The transferrin receptor: a potential molecular imaging marker for human cancer. *Neoplasia* **2003**, *5*, 495-506.

(29) Li, J. Y.; Paragas, N.; Ned, R.M.; Qiu, A.; Viltard, M.; Leete, T.; Drexler, I.R.; Chen, X.; Sanna-Cherchi, S.; Mohammed, F.; Williams, D.; Lin, C. S.; K.M. Schmidt-Ott, N.C. Andrews, J. Barasch. Scara5 is a ferritin receptor mediating non-transferrin iron delivery. *Dev Cell.* **2009**, *16*, 35-46.

(30) Mendes-Jorge, L.; Ramos, D.; Valença, A.; López-Luppo, M.; Pires, V. M.; Catita, J.; Nacher, V.; Navarro, M.; Carretero, A.; Rodriguez-Baeza, A.; Ruberte, J. L-ferritin binding to scara5: a new iron traffic pathway potentially implicated in retinopathy. *PloS One* **2014**, *9*, e106974.

(31) Falvo, E.; Tremante, E.; Fraioli, R.; Leonetti, C.; Zamparelli, C.; Boffi, A.; Morea, V.; Ceci, C.; Giacomini, P. Antibody-drug conjugates: targeting melanoma with cisplatin encapsulated in protein-cage nanoparticles based on human ferritin. *Nanoscale* **2013**, *5*, 12278-12285.

(32) Fan, K.; Gao, L.; Yan, X. Human ferritin for tumor detection and therapy. WIREs Nanomed Nanobiotechnol **2013**, *5*, 287-298.

(33) Fan, K.; Cao, C.; Pan, Y.; Lu, D.; Yang, D.; Feng, J.; Song, L.; Liang, M.; Yan, X. Magnetoferritin nanoparticles for targeting and visualizing tumour tissues. *Nature Nanotech.* **2012**, *7, 459–464.*

(34) Lin, X.; Xie, J.; Niu, G.; Zhang, F.; Gao, H.; Yang, M.; Quan, Q.; Aronova, M. A.; Zhang, G.; Lee S. *et al*. Chimeric ferritin nanocages for multiple function loading and multimodal imaging. *Nano Lett.* **2011**, *11*, 814-819.

(35) Liang, M.; Zhou, M.; Duan, D.; Zheng, J.; Yang, D.; Feng, J.; Yan, X. H-ferritin-nanocaged doxorubicin nanoparticles specifically target and kill tumors with a single dose injection. *Proc. Natl.. Acad. Sci*. **2011**, 41, 14900-14905.

(36) Ji, X. T.; Huang, L.; Huang, H. Q. Construction of nanometer cisplatin core-ferritin (NCC-F) and proteomic analysis of gastric cancer cell apoptosis induced with cisplatin released from the NCC-F. *J. Proteomics* **2012**, *75*, 3145-3157.

(37) Xing, R. M.; Wang, X. Y.; Zhang, C. L.; Zhang, Y. M.; Wang, Q.; Yang, Z.; Guo, Z. J. Characterization and cellular uptake of platinum anticancer drugs encapsulated in apoferritin. *J. Inorg. Biochem.* **2009**, *103*, 1039-1044.

(38) Ferraro, G.; Monti, D. M.; Amoresano, A.; Pontillo, N.; Petruk, G.; Pane, F.; Cinellu, M. A.; Merlino, A. Gold-based drug encapsulation within a ferritin nanocage: X-ray structure and biological evaluation as a potential anticancer agent of the Auox03-loaded protein. *Chem. Commun. (Camb)* **2016**, *52*, 9518-9521.

(39) Hulet, S. W.; Powers, S.; Connor, J. R. Distribution of transferrin and ferritin binding in normal and multiple sclerotic human brains. *J. Neurol. Sci.* **1999**, *165*, 48-55.

(40) Pontillo, N.; Pane, F.; Messori, L.; Amoresano, A.; Merlino, A. Cisplatin encapsulation within a ferritin nanocage: a high-resolution crystallographic study. *Chem. Commun. (Camb)* **2016**, *52*, 4136-4139.

(41) Tanley, S. W.; Diederichs, K.; Kroon-Batenburg, L. M.; Levy, C.; Schreurs, A. M.; Helliwell, J. R. Carboplatin binding to histidine. *Acta Crystallogr. F Struct. Biol. Commun*. **2014**, *70*, 1135-1142.

(42) Tanley, S. W.; Schreurs, A. M.; Kroon-Batenburg, L. M.; Helliwell, J. R. Re-refinement of 4xan: hen egg-white lysozyme with carboplatin in sodium bromide solution. *Acta Crystallogr. F Struct. Biol. Commun*. **2016**, *72*, 251-252

(43) Messori, L.; Marzo, T.; Merlino, A. Interactions of carboplatin and oxaliplatin with proteins: Insights from X-ray structures and mass spectrometry studies of their ribonuclease A adducts. *J. Inorg. Biochem.* **2015**, *153*, 136-142.

(44) Messori, L.; Merlino, A. Cisplatin binding to proteins: a stuctural perspective. *Coord. Chem. Rev.* **2016**, *315*, 67-89.

(45) Ferraro, G.; Massai, L.; Messori, L.; Merlino, A. Cisplatin binding to human serum albumin: a structural study. *Chem. Commun. (Camb).* **2015**, *51*, 9436-9439.

(46) Russo Krauss, I.; Ferraro, G.; Merlino, A. Cisplatin-Protein Interactions: Unexpected Drug Binding to N-Terminal Amine and Lysine Side Chains. *Inorg Chem*. **2016**, 55, 7814-7816.

(47) Messori, L.; Marzo, T.; Merlino, A. The X-ray structure of the complex formed in the reaction between oxaliplatin and lysozyme. *Chem. Comm.* **2014,** *50*, 8360-8362.

(48) Marasco, D.; Messori, L.; Marzo, T.; Merlino, A. Oxaliplatin vs. cisplatin: competition experiments on their binding to lysozyme. *Dalton Trans.* **2015,** *44*, 10392-10398.

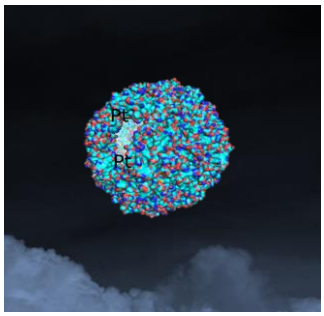

Table of Contents